AGU PUBLICATIONS

Geophysical Research Letters

RESEARCH LETTER

10.1002/2015GL064781

Special Section:
First Results from the MAVEN Mission to Mars

Key Points:
- MAVEN regularly observes energy-dispersed ions in the Martian magnetosphere
- Observed signatures are consistent with time dispersion, and often periodic
- The dispersion signatures can be produced by ion pickup in variable fields

Correspondence to:
J. S. Halekas,
jasper-halekas@uiowa.edu

Citation:
Halekas, J. S., et al. (2015), Time-dispersed ion signatures observed in the Martian magnetosphere by MAVEN, *Geophys. Res. Lett.*, *42*, doi:10.1002/2015GL064781.

Received 1 JUN 2015
Accepted 1 JUL 2015
Accepted article online 2 JUL 2015

Time-dispersed ion signatures observed in the Martian magnetosphere by MAVEN

J. S. Halekas[1], J. P. McFadden[2], J. E. P. Connerney[3], J. R. Espley[3], D. A. Brain[4], D. L. Mitchell[2], D. E. Larson[2], Y. Harada[2], T. Hara[2], S. Ruhunusiri[1], and B. M. Jakosky[4]

[1]Department of Physics and Astronomy, University of Iowa, Iowa City, Iowa, USA, [2]Space Sciences Laboratory, University of California, Berkeley, California, USA, [3]NASA Goddard Space Flight Center, Greenbelt, Maryland, USA, [4]Laboratory for Atmospheric and Space Physics, University of Colorado Boulder, Boulder, Colorado, USA

Abstract Mars Atmosphere and Volatile Evolution Mission's (MAVEN) high-cadence measurements reveal the frequent occurrence of ion energy dispersion events inside the Martian magnetosphere. The systematics of observed dispersion signatures suggest time dispersion of a broad source spectrum over a flight distance of a few thousand kilometers and disfavor mechanisms involving spatial dispersion. Pickup of heavy planetary ions in strong variable electric fields provides one potential mechanism that could produce the observed time dispersion signatures. The periodicity of many observed dispersion signatures, with frequencies near the upstream proton cyclotron frequency, suggests a possible role for low-frequency plasma waves in accelerating the observed ions from a source near the induced magnetospheric boundary to the observation location inside the magnetospheric tail lobes. The observed dispersion signatures may provide a new way to track the flow of energy from the upstream region through the magnetosphere and the role of waves in driving the escape of ions from the atmosphere.

1. Introduction and Context

The Martian magnetosphere, despite having almost entirely different physical origins from that of the Earth, shares many of the same features, including a bow shock, a magnetosheath, and an extended magnetotail with a central current sheet [*Nagy et al.,* 2003]. However, unlike at the Earth, heavy ions produced from the Martian atmosphere play a primary role in forming the obstacle to the solar wind flow, and the induced magnetospheric boundary (IMB) between the magnetosheath and the magnetosphere marks a compositional transition between a plasma mainly composed of solar wind protons and one composed of heavy planetary ions [*Rosenbauer et al.,* 1989; *Lundin et al.,* 1990; *Sauer et al.,* 1994].

Observations from Phobos-2, Mars Express, and Mars Global Surveyor have shown that the Martian magnetosphere is a highly dynamic environment, with very large fluctuations in density and fields [*Gurnett et al.,* 2010; *Halekas et al.,* 2011], which may result from a number of phenomena, including low-frequency oscillations [*Winningham et al.,* 2006; *Espley et al.,* 2004], magnetic reconnection [*Eastwood et al.,* 2008; *Dubinin et al.,* 2012], and shear-driven instabilities [*Gunell et al.,* 2008; *Penz et al.,* 2004]. These processes and others can also play a role in accelerating planetary ions to nonthermal velocities [*Dubinin et al.,* 2011].

Despite the induced nature of the Martian magnetosphere, spacecraft at Mars have observed a variety of processes also seen in the terrestrial magnetosphere. In this paper, we discuss dispersed ion signatures, not previously reported at Mars, but frequently seen in the terrestrial auroral zone [*Zelenyi et al.,* 1990] and magnetotail [*Savaud and Kovrazhkin*, 2004]. At Earth, these events result from at least two different processes, including spatial separation of a broad-spectrum source by energy-dependent drifts [*Bosqued et al.,* 1993] and temporal separation of a broad-spectrum source "injected" by a "convection surge" associated with dipolarizations in the tail and dispersed as they travel to the observer [*Mauk*, 1986; *Delcourt and Sauvaud*, 1994]. The latter mechanism can also lead to the occurrence of quasiperiodic "bouncing ion clusters" that repeatedly mirror on closed field lines [*Quinn and McIlwain*, 1979; *Keiling et al.,* 2005].

2. Ion Energy Dispersion Signatures Observed by Mars Atmosphere and Volatile Evolution Mission

Mars Express [*Barabash et al.,* 2007] and Phobos-2 [*Rosenbauer et al.,* 1989; *Lundin et al.,* 1990] have previously made ion measurements at Mars with highly capable instrumentation. However, Mars

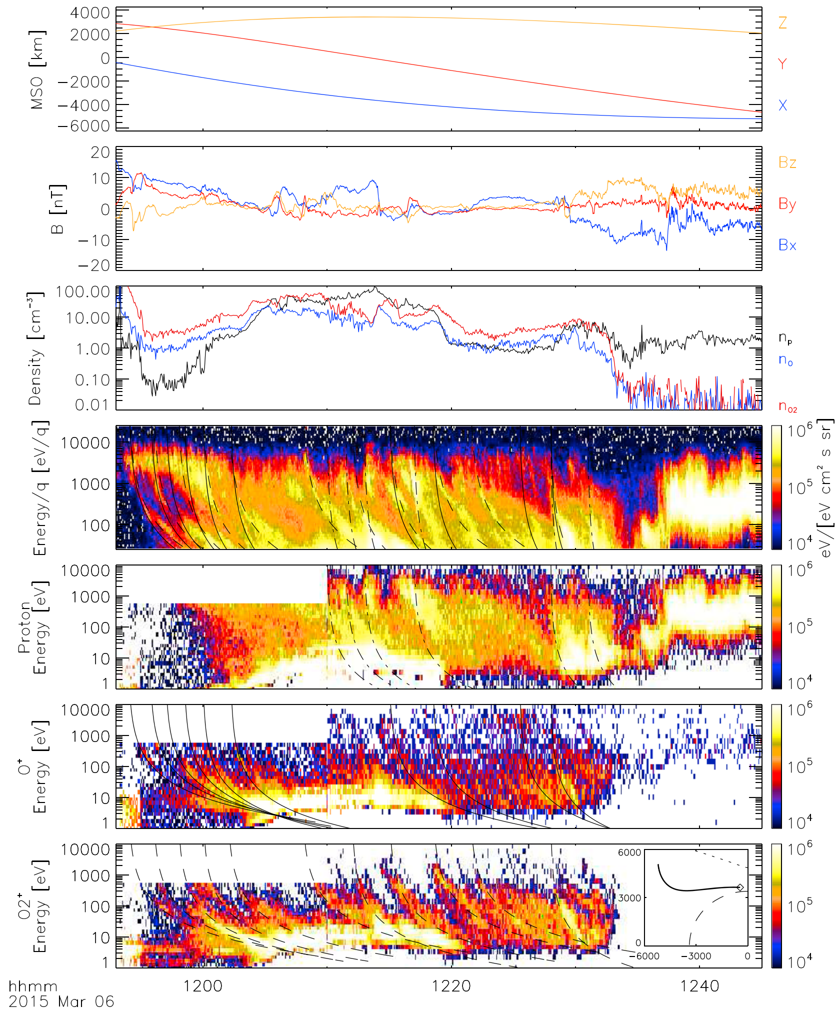

Figure 1. Spacecraft position in Mars Solar Orbital (MSO) magnetic field components in MSO, densities of major ion species measured by STATIC, ion omnidirectional differential energy flux spectra measured by SWIA, and corresponding spectra of protons, oxygen, and molecular oxygen ions measured by STATIC. Solid, dashed, and dash-dotted lines show time-of-flight dispersion curves calculated for O^+, O_2^+, and protons, with flight distance adjusted to roughly match observations (assumed distances range from 1000 to 4000 km]. The inset in the bottom panel shows a cylindrical projection of the spacecraft motion during this time period, with Mars and the nominal IMB position shown by dashed lines and a diamond marking the start time.

Express ion measurements had a 192 s cadence in the nominal operational mode. With Mars Atmosphere and Volatile Evolution Mission (MAVEN), measurement cadences as fast as 4 s for both the Solar Wind Ion Analyzer (SWIA) [*Halekas et al.,* 2013] and Suprathermal and Thermal Ion Composition (STATIC) [*McFadden et al.,* 2014] ion instruments allow new observations of rapidly varying ion fluxes such as those produced in dispersion events. Figures 1 and 2 show representative examples of two types of ion dispersion events frequently observed by MAVEN inside the IMB.

Figure 1 shows a complex set of dispersion events in the Martian magnetotail, identifiable in the omni-directional energy spectra from SWIA, and in three different mass ranges measured by the STATIC instrument. Angular spectra (not shown) indicate that most of the flux associated with these events is directed tailward, with a smaller off-axis component directed roughly toward the center of the magnetotail throughout the interval. All of the dispersion signatures in this event and in the vast majority of events observed to date have the proper sense for time dispersion of a broad spectrum produced at a distant location, inconsistent with spatial dispersion, which should on average produce as many “rising tones” as “falling tones” in the energy spectra.

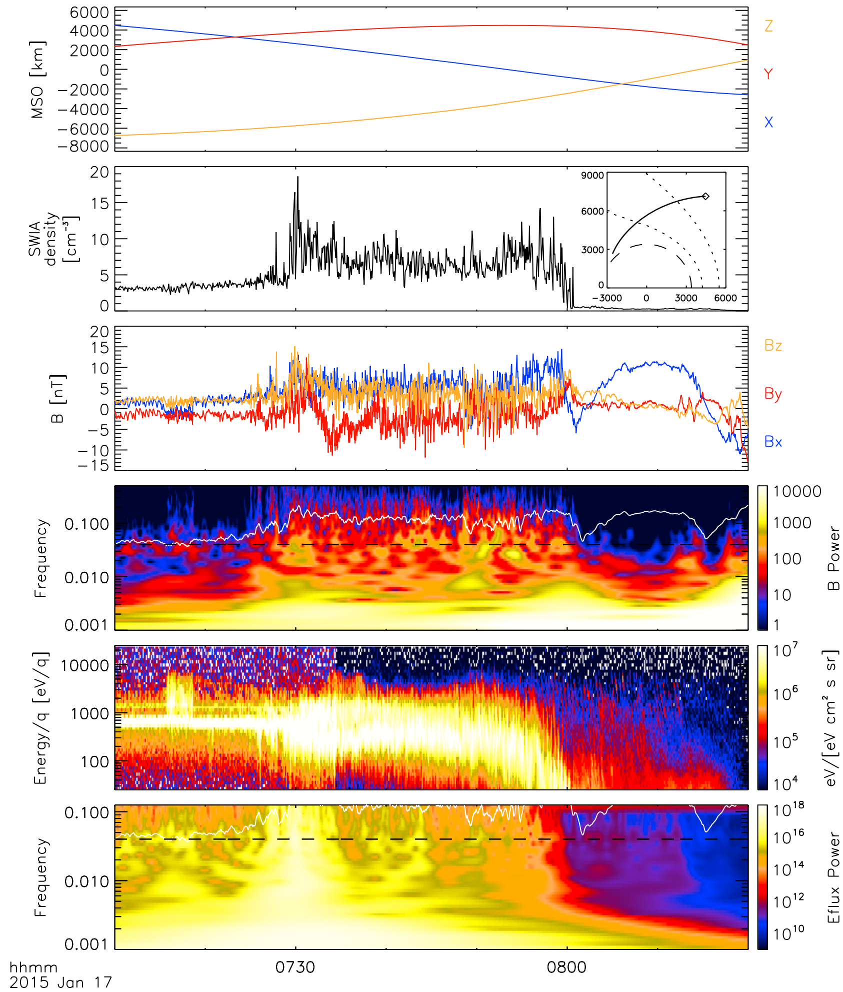

Figure 2. Spacecraft position in MSO coordinates, total density measured by SWIA for ions with energy/charge > 25 eV, magnetic field components in MSO, power spectral density of the magnetic field summed over all three components, ion omnidirectional differential energy flux spectra measured by SWIA, and power spectral density of measured differential energy flux, summed over energies of 200–5000 eV. The white line shows the local proton cyclotron frequency, and the dashed black line shows the upstream proton cyclotron frequency. The inset in the second panel shows a cylindrical projection of the spacecraft motion during this time period, with Mars and the nominal IMB and bow shock positions shown by dashed lines and a diamond marking the start time.

The signatures seen in the proton spectra appear on average steeper than those in the O^+ spectra, which in turn are steeper than those in the O_2^+ spectra, consistent with the expected 1/√M dependence for the velocity associated with a given energy per charge. The modeled dispersion signatures overlaid on the plots, which match the observations well in most cases, have no free parameters other than flight distance, with this parameter varying from ~4000 km early in the interval to ~1000–2000 km later in the interval. These time dispersion curves appear to fit the heavy ion signatures significantly better than those of the protons, suggesting that the protons may have had their energies modified to some degree while in flight from the source, that magnetic deflection may have played a preferential role given the smaller gyroradii of the protons, or that protons other than the dispersed populations also play a role.

Figure 2 shows a second orbit on which MAVEN observed a representative dispersion event just inside the IMB, with a somewhat different character. On this orbit, MAVEN passed from the solar wind (times before ~07:35) to the sheath (~07:35–07:55) and into the tail lobe (~8:05–8:15), encountering closely spaced dispersion signatures at energies from ~100 eV to ~5 keV near the IMB and in the lobe, from ~8:00 to 8:15. In this case, the time-dispersed signatures represent primarily tailward-moving heavy ions and display a very clear periodicity at ~0.05 Hz. The unidirectional nature of the observed fluxes strongly suggests that repeated mirroring could not

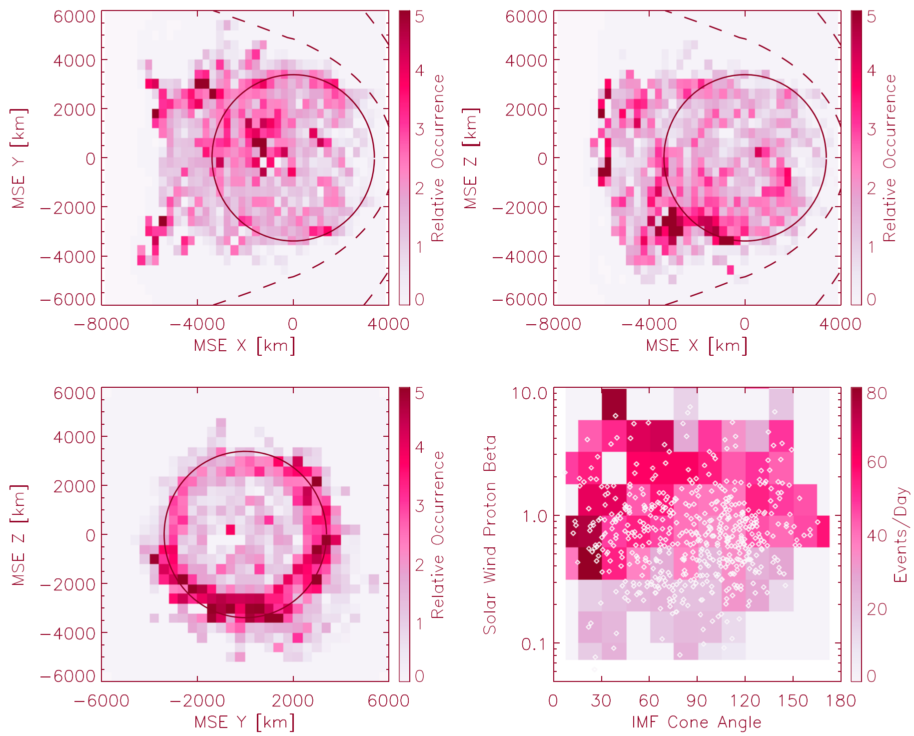

Figure 3. The first three panels show three projections in MSE coordinates of the relative occurrence frequency of time-dispersed ion events for the time period 27 November 2014 through 16 March 2015, calculated by dividing the normalized observation frequency by the normalized frequency with which MAVEN sampled each spatial bin. In MSE coordinates, the solar wind velocity lies along the $-X$ axis, the convection electric field lies along the Z axis, and the IMF lies in the X-Y plane with positive Y component. Dashed curves show the nominal positions of the bow shock and magnetic pileup boundary. The bottom right panel shows the number of events per day as a function of IMF cone angle (defined such that $+B_x$ corresponds to a cone angle of 0) and upstream solar wind proton beta [$n_p k T_p/(B^2/2\mu_0)$]. Each white diamond represents a single orbit average, so that the distribution of diamonds indicates the data density.

have produced the periodicity. Furthermore, this periodicity appears at the same frequency as fluctuations observed in the nearby magnetosheath population, as well as in the upstream solar wind, as shown by a power spectral analysis of ion differential energy fluxes for energies of 200–5000 eV.

We find that the observed periodicity closely corresponds to the upstream proton cyclotron frequency (but not the local proton cyclotron frequency) and that some power at this frequency also exists upstream and throughout the sheath in the magnetic field fluctuations. We observe a similar relationship between the upstream proton cyclotron frequency and the periodicity of time-dispersed ion signatures on many, but not all, such events. Though the mechanism for the propagation of the fluctuations through the sheath remains unclear, upstream waves associated with either hydrogen pickup ions or protons reflected from the bow shock may produce pressure pulses that perturb the bow shock [*Mazelle et al.*, 2004] and then propagate through the sheath. These fluctuations may then couple to heavy ions in some way to produce the periodic time-dispersed signatures that we observe. We will discuss a potential mechanism in more detail in section 4.

3. Distribution of Ion Dispersion Events

In order to investigate the systematics of the mechanisms responsible for producing the observed dispersion events, we used SWIA omnidirectional spectra to visually identify 4391 dispersion events during the time range from 27 November 2014 to 16 March 2015. The complex and overlapping nature of events such as those shown in Figure 1 makes separation of discrete events challenging and subject to interpretation, but the resulting distribution should at least show the broad systematics of the occurrence of dispersion events. Figure 3 shows the relative probability of observing the identified dispersion signatures, in Mars Solar Electric (MSE) coordinates organized by the upstream solar wind velocity from SWIA measurements and the

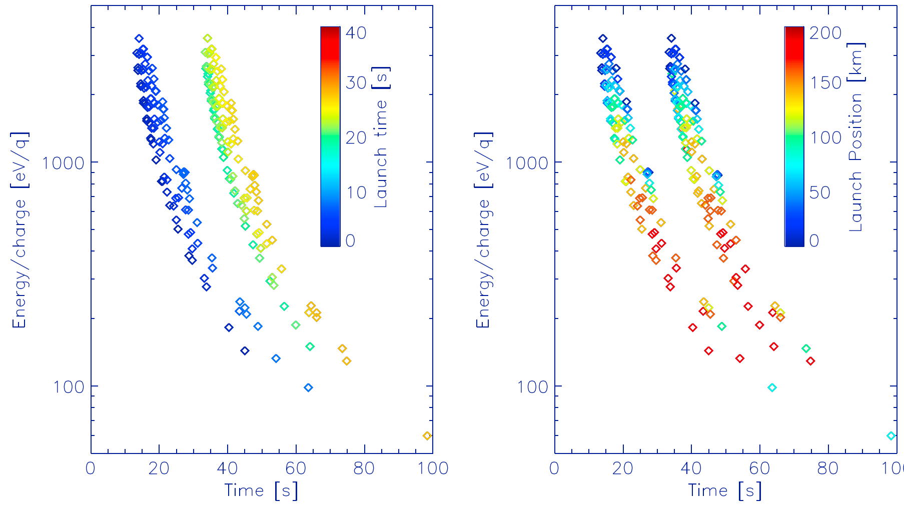

Figure 4. Observed energy as a function of time for O^+ pickup ions injected with a uniform production rate in a slab 200 km thick, subjected to two periods of an electric field uniform throughout the slab, but varying sinusoidally in time, with amplitude of 18 mV/m and frequency of 0.05 Hz, and then measured 1800 km from the nearest point of the source region. The colors on the left and right panels show the ionization time and the position of ionization in the slab for each ion.

interplanetary magnetic field (IMF) measured by the Magnetometer (MAG) [*Connerney et al.,* 2015]. We find that the great majority of events take place well inside the nominal IMB, with the highest probability of observation near the light-shadow boundary, in the hemisphere opposite to the solar wind convection electric field (the −E hemisphere). In this hemisphere, the electric field points inward toward the center of the magnetotail, suggesting a possible source near the IMB and propagation inward to the observation location.

The probability distributions of upstream density and magnetic field for orbits with dispersion events do not differ radically from those for orbits without dispersion events; however, statistical trends do exist, as shown in Figure 3 (bottom right). Dispersion events occur preferentially during orbits with high upstream solar wind proton beta (computed from SWIA and MAG measurements), perhaps implying that ion-driven waves produced upstream may play a role in the formation of the dispersed ion signatures. We also note a preference for cone angles near 0 and 180, which may also favor the growth and propagation of upstream waves. Finally, one can identify some clustering of high occurrence rates for $+B_x$, but this simply recapitulates the preference for occurrence in the −E hemisphere, given the MAVEN periapsis in the northern geographic hemisphere throughout the interval in question.

4. Ion Pickup in Quasiperiodic Electric Fields

A number of scenarios for ion velocity dispersion have been discussed in the context of the terrestrial magnetosphere. At Mars, some of these scenarios, such as dipolarization of the magnetotail, do not appear viable, given the predominantly open-field geometry of the Martian tail. The systematics of the observed events provides us with some clues that may help us understand why these dispersion events occur. First, since the vast majority of observed dispersion signatures show energies that decrease as a function of time, regardless of the IMF geometry or orbit phase, scenarios involving spatial dispersion due to energy-dependent drifts most likely do not play a significant role. Instead, time dispersion of a source population appears likely, in which case the problem becomes how to inject a broad spectrum at a given location.

In this case, the primarily heavy ion composition and the quasiperiodicity of the observed signatures provide us with potentially important clues. One way to produce an effectively broad spectrum is to subject low-energy ions, such as those produced from photo-ionization and charge exchange, to a force that varies over short timescales. If one could apply this force in a periodic fashion, one could generate periodic bursts of ions with a range of energies, which would then disperse in time as they traveled from the source location to the observation point. To test the viability of this hypothesis, we conducted a very simple simulation of ion pickup with a uniform production rate in a small region exposed to a sinusoidally varying electric field (in the planetary frame). After allowing the resulting accelerated particles to disperse over a long flight path, as shown in Figure 4, we found energy-time characteristics very similar to those actually observed. We also simulated both lighter and heavier ions, finding similar signatures, but with more (less) time dispersion for heavier (lighter) ions, commensurate with the smaller (greater) speeds for the same energy per charge. At the scales simulated, all ions remain unmagnetized during their acceleration, but protons could experience significant magnetic deflection between the acceleration region and the observation location, possibly explaining the deviation from perfect dispersion curves observed in Figure 1.

This model implies that newly born pickup ions that experience a strong variable electric field could explain the observed time dispersion signatures. If correct, such a model requires either a large source volume or a strong electric field, on the order of 8 times larger than the nominal solar wind convection electric field for the case simulated in Figure 4, or less if the acceleration region has a larger scale. The flank magnetosheath provides one likely location for such strong electric field pulsations, given the large observed magnetic field compression ratios, but only slightly decelerated ion flows. The preference for IMF cone angles near 0 and 180 does not obviously support this hypothesis, but even for cone angles of ~30 or ~150, significant convection electric fields can exist. Near the IMB, there should be a high enough production rate of heavy planetary pickup ions exposed to these driving electric fields to produce the signatures we observe. In this scenario, the preponderance of observations in the −E hemisphere might indicate that we can more easily observe newly born ions driven into the low-density magnetospheric tail lobes, whereas those produced in the +E hemisphere travel outward into the sheath, where we cannot easily observe them. Alternatively, assuming the waves in question originate upstream as suggested by the class of events shown in Figure 2, it may indicate that strong waves capable of driving ion acceleration can more easily transfer energy inward from the bow shock to the IMB in the −E hemisphere.

5. Implications and Conclusions

MAVEN's high-cadence ion observations provide a new window on dynamic processes in the Martian magnetosphere. While energy-dispersed ions commonly occur in the terrestrial magnetosphere, we are unaware of previous reports of such phenomena at Mars. With MAVEN, however, we find that ion energy dispersion occurs very frequently inside the Martian IMB, with the systematics of the observed signatures supporting time dispersion of a broad source spectrum over a flight distance of a few thousand kilometers. While similar processes operate regularly in the terrestrial magnetosphere, at Mars the mechanism for producing the broad source spectrum most likely must differ from the processes that operate at the Earth. We suggest herein that ion pickup in strong variable electric fields could produce the observed signatures. Low-frequency plasma waves generated upstream and driving pressure pulses across the bow shock provide one potential driver for such variable electric fields, and the preponderance of fluctuations at the upstream proton cyclotron frequency supports this hypothesis. Previously, *Ergun et al.* [2006] and *Lundin et al.* [2011] have discussed a role for similar waves produced in and/or convecting through the sheath in heating ionospheric ions at low altitudes. Our observations may in fact represent an imprint of the high-altitude extension of this process. If so, future studies should explore the role of these same waves at lower altitudes and determine whether we can use the observed dispersion signatures to help track the flow of energy through the Martian system and the subsequent escape of ions from the atmosphere. Finally, the time-dispersed ions themselves constitute an escaping population, which should be placed into context with the other escape channels from the Martian atmosphere.

Acknowledgments
We acknowledge the efforts of a terrific team of engineers and scientists over more than a decade to make the MAVEN mission and its state-of-the-art instrumentation a reality. MAVEN data are publicly available through the Planetary Data System.

The Editor thanks Cesar Bertucci and Eduard Dubinin for their assistance in evaluating this paper.

References

Barabash, S., et al. (2007), The Analyzer of Space Plasmas and Energetic Atoms (ASPERA-3) for the Mars Express mission, *Space Sci. Rev.*, doi:10.1007/s11214-006-9124-8.

Bosqued, J. M., et al. (1993), Dispersed ion structures at the poleward edge of the auroral oval: Low-altitude observations and numerical modeling, *J. Geophys. Res.*, *98*, 19,181–19,204, doi:10.1029/93JA01143.

Connerney, J., J. Espley, P. Sheppard, and R. O. Lawton (2015), The MAVEN magnetic field investigation, *Space. Sci. Rev.*, doi:10.1007/s11214-015-0169-4.

Delcourt, D. C., and J.-A. Sauvaud (1994), Plasma sheet ion energization during depolarization events, *J. Geophys. Res.*, *99*, 97–108, doi:10.1029/93JA01895.

Dubinin, E., M. Fraenz, A. Fedorov, R. Lundin, N. Edberg, F. Duru, and O. Vaisberg (2011), Ion energization and escape on Mars and Venus, *Space Sci. Rev.*, *162*, 173–211.

Dubinin, E., M. Fraenz, J. Woch, T. L. Zhang, J. Wei, A. Fedorov, S. Barabash, R. Lundin (2012), Bursty escape fluxes in plasma sheets of Mars and Venus, *Geophys. Res. Lett.*, *39*, L01104, doi:10.1029/2011GL049883.

Eastwood, J. P., D. A. Brain, J. S. Halekas, J. F. Drake, T. D. Phan, M. Øieroset, D. L. Mitchell, R. P. Lin, and M. Acuña (2008), Evidence for collisionless magnetic reconnection at Mars, *Geophys. Res. Lett.*, *35*, L02106, doi:10.1029/2007GL032289.

Ergun, R. E., L. Andersson, W. K. Peterson, D. Brain, G. T. Delory, D. L. Mitchell, R. P. Lin, and A. W. Yau (2006), Role of plasma waves in Mars' atmospheric loss, *Geophys. Res. Lett.*, *33*, L14103, doi:10.1029/2006GL025785.

Espley, J. R., P. A. Cloutier, D. A. Brain, D. H. Crider, and M. H. Acuña (2004), Observations of low-frequency magnetic oscillations in the Martian magnetosheath, magnetic pileup region, and tail, *J. Geophys. Res.*, *109*, A07213, doi:10.1029/2003JA010193.

Gunell, H., et al. (2008), Shear driven waves in the induced magnetosphere of Mars, *Plasma Phys. Control Fusion*, *50*, doi:10.1088/0741-3335/50/7/074018.

Gurnett, D. A., et al. (2010), Large density fluctuations in the Martian ionosphere as observed by the Mars Express radar sounder, *Icarus*, *206*, 83, doi:10.1016/j.icarus.2009.02.019.

Halekas, J. S., D. Brain, and J. P. Eastwood (2011), Large amplitude compressive "sawtooth" magnetic field oscillations in the Martian magnetosphere, *J. Geophys. Res.*, *116*, A07222, doi:10.1029/2011JA016590.

Halekas, J. S., E. R. Taylor, G. Dalton, G. Johnson, D. W. Curtis, J. P. McFadden, D. L. Mitchell, R. P. Lin, and B. M. Jakosky (2013), The solar wind ion analyzer for MAVEN, *Space Sci. Rev.*, doi:10.1007/s11214-013-0029-z.

Keiling, A., et al. (2005), Bouncing ion clusters in the plasma sheet boundary layer observed by Cluster-CIS, *J. Geophys. Res.*, *110*, A09207, doi:10.1029/2004JA010497.

Lundin, R., A. Zakharov, R. Pellinen, H. Borg, B. Hultqvist, N. Pissarenko, E. M. Dubinin, S. W. Barabasj, I. Liede, and H. Koskinen (1990), Plasma composition measurements of the Martian magnetosphere morphology, *Geophys. Res. Lett.*, *17*, 877, doi:10.1029/GL017i006p00877.

Lundin, R., S. Barabash, E. Dubinin, D. Winningham, M. Yamauchi (2011), Low-altitude acceleration of ionospheric ions at Mars, *Geophys. Res. Lett.*, *38*, L08108, doi:10.1029/2011GL047064.

Mauk, B. H. (1986), Quantitative modeling of the "convection surge" mechanism of ion acceleration, *J. Geophys. Res.*, *91*, 13,423–13,431, doi:10.1029/JA091iA12p13423.

Mazelle, C., et al. (2004), Bow shock and upstream phenomena at Mars, *Space Sci. Rev.*, *11*, 115.

McFadden, J., et al. (2014), The MAVEN Suprathermal and Thermal Ion Composition (STATIC) instrument, *Space Sci. Rev.*

Nagy, A., et al. (2003), The plasma environment of Mars, *Space Sci. Rev.*, *111*, 33.

Penz, T., et al. (2004), Ion loss on Mars caused by the Kelvin-Helmholtz instability, *Planet. Space Sci.*, *52*, 1157–1167.

Quinn, J. M., and C. E. McIlwain (1979), Bouncing ion clusters in the Earth's magnetosphere, *J. Geophys. Res.*, *84*, 7365–7370, doi:10.1029/JA084iA12p07365.

Rosenbauer, H., et al. (1989), Ions of Martian origin and plasma sheet in the Martian magnetosphere: Initial results of the TAUS experiment, *Nature*, *341*, 612.

Sauer, K., A. Bogdanov, and K. Baumgartel (1994), Evidence of an ion composition boundary (protonopause) in bi-ion fluid simulations of solar wind mass loading, *Geophys. Res. Lett.*, *21*, 2255–2258, doi:10.1029/94GL01691.

Savaud, J.-A. and R. A. Kovrazhkin (2004), Two types of energy-dispersed ion structures at the plasma sheet boundary, *J. Geophys. Res.*, *109*, A12213, doi:10.1029/2003JA010333.

Winningham, J. D., et al. (2006), Electron oscillations in the induced Martian magnetosphere, *Icarus*, *182*, 360–370.

Zelenyi, L. M., R. A. Kovrazhkin, and J. M. Bosqued (1990), Velocity- dispersed ion beams in the nightside auroral zone: AUREOL 3 observations, *J. Geophys. Res.*, *95*, 12,119–12,139, doi:10.1029/JA095iA08p12119.